



HAL
open science

The deletion of the microtubule-associated STOP protein affects the serotonergic mouse brain network.

Vincent Fournet, Marion Jany, Véronique Fabre, Farah Chali, Didier Orsal, Annie Schweitzer, Annie Andrieux, Fany Messanvi, Bruno Giros, Michel Hamon, et al.

► To cite this version:

Vincent Fournet, Marion Jany, Véronique Fabre, Farah Chali, Didier Orsal, et al.. The deletion of the microtubule-associated STOP protein affects the serotonergic mouse brain network.. *Journal of Neurochemistry*, 2010, 115 (6), pp.1579-94. 10.1111/j.1471-4159.2010.07064.x . inserm-00566974

HAL Id: inserm-00566974

<https://inserm.hal.science/inserm-00566974>

Submitted on 17 Feb 2011

HAL is a multi-disciplinary open access archive for the deposit and dissemination of scientific research documents, whether they are published or not. The documents may come from teaching and research institutions in France or abroad, or from public or private research centers.

L'archive ouverte pluridisciplinaire **HAL**, est destinée au dépôt et à la diffusion de documents scientifiques de niveau recherche, publiés ou non, émanant des établissements d'enseignement et de recherche français ou étrangers, des laboratoires publics ou privés.

The deletion of the microtubule-associated STOP protein affects the serotonergic mouse brain network

Vincent Fournet,^{*,†,1} Marion Jany,^{†,1} Véronique Fabre,[‡] Farah Chali,^{*} Didier Orsal,^{*} Annie Schweitzer,[†] Annie Andrieux,[†] Fany Messanvi,^{*} Bruno Giros,^{*} Michel Hamon,[§] Laurence Lanfumey,[§] Jean-Christophe Deloulme[†] and Marie-Pascale Martres^{*}

^{*}INSERM UMRS 952, CNRS UMR 7224, Université Pierre et Marie Curie, Paris, France

[†]INSERM U836, Grenoble Institut Neurosciences, CEA-iRTSV-GPC, Université Joseph Fourier, Grenoble, France

[‡]INSERM UMRS 975, Université Pierre et Marie Curie, Paris, France

[§]INSERM UMRS 894, Université René Descartes, Paris, France

Abstract

The deletion of microtubule-associated protein stable tubule only polypeptide (STOP) leads to neuroanatomical, biochemical and severe behavioral alterations in mice, partly alleviated by antipsychotics. Therefore, STOP knockout (KO) mice have been proposed as a model of some schizophrenia-like symptoms. Preliminary data showed decreased brain serotonin (5-HT) tissue levels in STOP KO mice. As literature data demonstrate various interactions between microtubule-associated proteins and 5-HT, we characterized some features of the serotonergic neurotransmission in STOP KO mice. In the brainstem, mutant mice displayed higher tissue 5-HT levels and *in vivo* synthesis rate, together with marked increases in 5-HT transporter densities and 5-HT_{1A} autoreceptor levels and electrophysiological sensitivity, without modification of the serotonergic soma number. Conversely, in

projection areas, STOP KO mice exhibited lower 5-HT levels and *in vivo* synthesis rate, associated with severe decreases in 5-HT transporter densities, possibly related to reduced serotonergic terminals. Mutant mice also displayed a deficit of adult hippocampal neurogenesis, probably related to both STOP deletion and 5-HT depletion. Finally, STOP KO mice exhibited a reduced anxiety- and, probably, an increased helplessness-status, that could be because of the strong imbalance of the serotonin neurotransmission between somas and terminals. Altogether, these data suggested that STOP deletion elicited peculiar 5-HT disconnectivity.

Keywords: anxiety/depression, electrophysiology, neurogenesis, schizoaffective disorders, stable tubule only polypeptide, STOP KO mice.

J. Neurochem. (2010) **115**, 1579–1594.

Neuronal microtubules have major central functions as progenitor division, neuronal morphogenesis or differentiation and axonal transport. In line with the probable involvement of neuronal cytoskeleton disorganization in psychiatric disorders (Robertson *et al.* 2006; Ross *et al.* 2006; Talbot *et al.* 2006; Camargo *et al.* 2007; Desbonnet *et al.* 2009), mice lacking the protein STOP (stable tubule only polypeptide knock out, STOP KO, Andrieux *et al.* 2002), a microtubule-associated protein (MAP) essential for neuronal morphogenesis and maintenance (Bosc *et al.* 1996; Guillaud *et al.* 1998), display many characteristics, considered to be landmarks of schizophrenia (Frankle *et al.* 2003).

STOP KO mice exhibit brain anatomical abnormalities such as enlarged ventricles and reduced cortical and diencephalic volumes (Powell *et al.* 2007). They show

Received May 21, 2010; revised manuscript received October 8, 2010; accepted October 13, 2010.

Address correspondence and reprint requests to Marie-Pascale Martres, INSERM UMRS 952, CNRS UMR 7224, Université Pierre et Marie Curie, Physiopathologie des maladies du système nerveux central, 9 Quai Saint Bernard, case courrier 37, 75252 Paris cedex 5, France. E-mail: marie-pascale.martres@snv.jussieu.fr

¹These authors contributed equally to this study.

Abbreviations used: 5-HIAA, 5-hydroxyindolacetic acid; 5-HT, serotonin; 5-HTP, 5-hydroxytryptophan; aCSF, artificial CSF; BrdU, 5-bromo-2'-deoxyuridine; DA, dopamine; DCX, doublecortin; DISC1, disrupted in schizophrenia 1; DR, dorsal raphe; i.p., intra peritoneal; KO, knockout; MAP, microtubule-associated protein; SERT, serotonin transporter; SGZ, subgranular zone; STOP, stable tubule only polypeptide; SVZ, subventricular zone; TPH2, tryptophan hydroxylase 2; WT, wild-type.

hyperdopaminergia in the limbic system evidenced by an increased dopamine (DA) evoked efflux in the nucleus accumbens (Brun *et al.* 2005), a decreased DA uptake by accumbens synaptosomes, a lower level of D₂ and D₃ DA receptors in some brain areas (Bouvrais-Veret *et al.* 2008) and an increased glucose utilization in the DA cell body areas (Hanaya *et al.* 2008). Mutant mice also exhibit a probable hypoactivity of glutamatergic neurotransmission characterized by a decreased number of hippocampal synaptic vesicles and a deficit in the long term potentiation (Andrieux *et al.* 2002), a decreased vesicular glutamate transporter 1 mRNA level in hippocampus (Eastwood *et al.* 2007) and an increased glutamine metabolism (Brenner *et al.* 2007). STOP KO mice show purposeless and disorganized activity, impaired social interactions and maternal behavior (Andrieux *et al.* 2002; Begou *et al.* 2008). They are hypersensitive to the locomotor effect of mild stress and of psychostimulants as amphetamine, nicotine and cocaine (Brun *et al.* 2005; Bouvrais-Veret *et al.* 2007, 2008). Mutant mice are deficient in sensory-gating mechanisms (Fradley *et al.* 2005) and learning performance in the novel object recognition and olfactory discrimination tasks (Powell *et al.* 2007; Begou *et al.* 2008) and in the cued version of the Morris watermaze test (Bouvrais-Veret *et al.* 2007). Importantly, some symptoms appear post-pubertally (Begou *et al.* 2007) and part of dysfunctions are alleviated by chronic treatment with antipsychotics (Andrieux *et al.* 2002; Brun *et al.* 2005; Delotterie *et al.* 2009). Finally, the gene encoding MAP6, the human homolog of STOP, is localized on chromosome 11q14, a region highly associated with schizotypal personality disorders (Lewis *et al.* 2003) and an association between MAP6 gene polymorphism and schizophrenia has been reported (Shimizu *et al.* 2006).

Preliminary data on STOP KO mice showed significant alterations in brain levels of monoamines, including DA (Bouvrais-Veret *et al.* 2008) and serotonin (5-HT). Interactions between some neurotransmitters and MAPs have been reported at both the transcriptional and post-transcriptional levels. Concerning the serotonergic neurotransmission, convergent studies showed that (i) serotonin depletion in rats triggers a loss of MAP2 in hippocampal dendrites (Whitaker-Azmitia *et al.* 1995), (ii) acute or chronic antidepressant treatments with selective serotonin reuptake inhibitors stimulate microtubule dynamics in the rat hippocampus (Perez *et al.* 1995; Bianchi *et al.* 2009) and (iii) selective MAPs colocalize in cortical dendrites or directly interact with some serotonin receptors (Cornea-Hébert *et al.* 1999, 2002; Sun *et al.* 2008). Interestingly, epidemiologic studies showed co-segregation of schizophrenia and mood disorders within families (Laursen *et al.* 2005; Gottesman *et al.* 2010) and recent genetic investigations point at various susceptibility genes common to these psychiatric disorders, such as those encoding DISC1 (disrupted-in-schizophrenia1), neu-

regulin 1, dysbindin-1 and catechol-*O*-methyltransferase (Craddock and Forty 2006). Finally, mice with mutations in the DISC1 gene exhibit phenotype related to either schizophrenia or depression, depending on the location of the punctual mutation (Clapcote *et al.* 2007).

For all these reasons, we investigated the effects of the microtubule-associated STOP protein deletion on various parameters of serotonergic neurotransmission in STOP KO mice, using molecular, anatomical, physiological and behavioral approaches. Altogether, our results showed that STOP deletion triggers dramatic alterations of the serotonin neurotransmission, with marked imbalance of 5-HT tone in brainstem vs. forebrain areas and associated consequences on adult hippocampal neurogenesis and on anxiety- and depression-related behaviors.

Materials and methods

Animals

Stable tubule only polypeptide deficient mice were obtained by putting the lacZ gene in the place of the exon 1 of STOP gene (MAP6, Denarier *et al.* 1998), present in all characterized STOP isoforms (A-, E-, F-, N- and O-STOP, Aguezzoul *et al.* 2003; Galiano *et al.* 2004). Thus, the exon 1 deletion results in the absence of any detectable STOP isoforms in STOP KO mice (Andrieux *et al.* 2002). Homozygous wild-type (WT) mice and STOP KO littermates were obtained by crossing (F2) heterozygous 50 : 50 BALBc/129 SvPas-F1 and genotyped as previously described (Andrieux *et al.* 2002). Animals were kept under standard conditions, with a 12 h light/dark cycle (lights on at 07:30 h) and allowed to habituate to the animal holding room for at least 1 week prior to use. All experiments were conducted on WT and STOP KO mice of the same litters and at 3–5 months of age, in accordance with the European Communities Council directive (86/809/EEC).

Drugs

5-Bromo-2'-deoxyuridine (BrdU), clorgiline hydrochloride, 5-hydroxytryptamine hydrochloride (5-HT, serotonin), fluoxetine hydrochloride and 3-hydroxy-benzylhydrazine (NSD 1015) were purchased from Sigma-Aldrich (Saint Quentin-Fallavier, France). Venlafaxine hydrochloride was from Tocris (Bristol, UK) and ipsapirone hydrochloride from Bayer-Troponwerke (Cologne, Germany). BrdU, clorgiline, NSD 1015 and venlafaxine were dissolved in 0.9% NaCl and administered intraperitoneally (100 µL per 10 g body weight). Polyclonal antibodies against rabbit anti-5-HT were from Calbiochem (La Jolla, CA, USA), rabbit anti-tryptophan hydroxylase 2 (TPH2) and guinea pig anti-doublecortin (DCX) from Chemicon (Temecula, CA, USA), rat anti-BrdU from Abcys (Paris, France), mouse anti-Mash1 from BD Pharmingen (Franklin Lakes, NJ, USA), mouse anti-NeuN from Millipore (Molsheim, France) and rabbit anti-β-galactosidase from Rockefeller (New York, NY, USA). [³H]Citalopram (2.22–3.18 TBq/mmol) and [methoxy-³H]WAY 100635 (2.22–3.18 TBq/mmol) were purchased from GE Healthcare (Orsay, France) and [¹²⁵I]-IgG (74–370 kBq/µg, 9 kBq/mL) from Perkin Elmer (Orsay, France).

Determination of 5-HT, 5-hydroxytryptophan and 5-hydroxyindolacetic acid tissue levels and of *in vivo* tryptophan hydroxylase activity

The concentrations of endogenous 5-HT, its precursor 5-hydroxytryptophan (5-HTP) and its metabolite 5-hydroxyindolacetic acid (5-HIAA) were determined by HPLC and electrochemical detection as previously reported (Bouvrais-Veret *et al.* 2008). After centrifugation and neutralization, 10 μ L-aliquots of brain homogenates were injected into a HPLC column (Ultrasphere IP, Beckman, Villepinte, France; 25 \times 4.6 cm, C18 reversed-phase, particle size 5 μ m). The mobile elution phase (flow rate: 1 mL/min) consisted of 70 mM KH₂PO₄, 2.1 mM triethylamine, 0.1 mM EDTA, 1.25 mM octane sulphonate and 16% methanol, adjusted to pH 3.02. The electrochemical detection system (ESA 5011, Bedford, MA, USA) comprises an analytical cell with dual coulometric monitoring electrodes (+50 mV and +350 mV).

For the *in vivo* measurement of TPH2 activity, animals received 100 mg/kg NSD 1015 intra peritoneal (i.p.), to block aromatic L-amino acid decarboxylase, and were killed 30 min later. Accumulated 5-HTP levels were measured as described above.

Autoradiographic labelings

Mice were killed by cervical dislocation and their brains frozen in isopentane at -30°C . Serial 10 μ m coronal sections were cut at -20°C , thaw-mounted on Superfrost Plus[®] slides (Mensch-Glaser, Braunschweig, Germany) and stored at -80°C until use.

Radiolabeling of 5-HT transporter and 5-HT1A receptors

Labeling of the 5-HT transporter (SERT) was performed according to Fabre *et al.* (2000b), by incubating slides for 60 min at 22°C in 50 mM Tris-HCl buffer, pH 7.4, containing 120 mM NaCl, 5 mM KCl and 2.5 nM [³H]citalopram, without or with 10 μ M fluoxetine to determine non-specific binding. Sections were then washed, dried and exposed to BAS-TR Fuji Imaging screen (Fujifilm Europe, GmbH, Dusseldorf, Germany) for 1 week. Labeling of 5-HT1A receptors was done as previously reported (Fabre *et al.* 2000a), by incubating sections for 60 min at 22°C in 100 mM Tris-HCl buffer, pH 7.4, containing 2 nM [methoxy-³H]WAY 100635, without or with 10 μ M 5-HT to determine non-specific binding. After washes and drying, sections were exposed to BAS-TR Fuji Imaging screen for 3 weeks.

Autoradiographic quantification

Standard radioactive microscales were exposed onto each Imaging screen to ensure that labeling densities were in the linear range. The screens were scanned with a Fuji Bioimaging Analyzer BAS-5000 and the densitometry performed with MCIDTM analysis software. Specific labelings of four sections per area were averaged per mouse.

Electrophysiological recordings

Extracellular recordings of dorsal raphe 5-HT neurons were performed on slices as previously reported (Mannoury la Cour *et al.* 2001). The mouse brains were immersed in an ice-cold artificial CSF (aCSF) containing 126 mM NaCl, 3.5 mM KCl, 1.2 mM NaH₂PO₄, 1.3 mM MgCl₂, 2 mM CaCl₂, 25 mM NaHCO₃ and 11 mM D-glucose, maintained at pH 7.3 by continuous bubbling with carbogen (95% O₂/5% CO₂) for 1 h at 22°C . Then, 400 μ m-coronal sections were placed on a nylon mesh and superfused

continuously with oxygenated aCSF (34°C , 2–3 mL/min). Extracellular recordings were made with glass microelectrodes filled with 2 M NaCl (10–15 M Ω). Baseline activity was recorded for 5–10 min before the application of the 5-HT1A receptor agonist ipsapirone (0–100 nM). The integrated firing rate was computed as consecutive 10 s samples. The effect of ipsapirone was evaluated by comparing the mean discharge frequency during 2 min before its addition with that recorded at the peak of its action, that is, 3–10 min after starting ipsapirone infusion.

Immunohistochemistry

Mice received an i.p. injection of 10 mg/kg clorgyline 3 h before anesthesia by sodium pentobarbital (80 mg/kg, i.p.) and were perfused transcardially with 4% paraformaldehyde. After post-fixation overnight, 30 μ m-coronal sections were cut using a vibratome.

After treatment with 3% H₂O₂, free-floating sections were pre-incubated in phosphate-buffered saline containing 4% bovine serum albumin and 0.1% Triton X-100 for 1 h at 22°C . Sections were incubated overnight at 4°C with polyclonal antibodies against 5-HT (1 : 100 000), TPH2 (1 : 1500), or SERT (1 : 3600, a generous gift of R.D. Blakely). Sections were then immunolabeled by the immunoperoxidase method as previously described (Bernard *et al.* 2008).

Serotonin soma counting and fiber density determination

For each mouse, 5-HT- and TPH2-immunoreactive neurons were counted within the dorsal raphe (DR) and the median raphe nuclei (Bregma -4.16 to -5.02 , according to Franklin and Paxinos 1997) and SERT-immunoreactive fiber density was measured within the dorsal dentate gyrus (Bregma -2.06 to -1.46) and the cingulate cortex (Cg Cx, Bregma 1.10 to 1.70). Sections were observed under bright field illumination and the resultant signals were quantified using the cell counting software Mercator Lite 3.0B (Explora Nova, La Rochelle, France) or the multi length and surface measure functions of the software Image J (NIH, Bethesda, MD, USA). All the cell counts, the fiber lengths and the surface areas were measured using an optic microscope (Zeiss Axioscop 2 plus, Le Pecq, France) at 40 \times magnification and a RVB camera (Zeiss Axiocam, Le Pecq, France). The number of 5-HT- and TPH2-positive cells, within the DR and the median raphe, was determined in seven different coronal sections, 120 μ m apart, and were averaged per region and per mouse. To avoid false double counting, only cells with nucleus were taken into account. The SERT-immunoreactive fiber lengths were determined in 10 microscopic fields randomly selected per section, corresponding to 10% of the dentate gyrus or the Cg Cx, in five different coronal sections, 120 μ m apart, without considering the intensity of staining. The fiber densities, calculated as the ratio of the total fiber lengths over the total surface of the microscopic fields, were finally averaged per region and per mouse.

Quantitative determination of neurogenesis

To analyze cell proliferation, mice were i.p. injected with 100 mg/kg BrdU, twice a day for 2 days and killed on the third day. To analyze neurogenesis and survival, mice received 50 mg/kg BrdU twice a day for 4 days and were killed 6 weeks later. After perfusion with 4% paraformaldehyde, the brains were cryoprotected in 30% sucrose and coronal free-floating sections were collected.

For immunofluorescence, labelings were performed as previously described (Raponi *et al.* 2007) using rat anti-BrdU (1 : 500), mouse anti-Mash1 (1 : 100), guinea pig anti-DCX (1 : 2000), mouse anti-NeuN (1 : 4000) and rabbit anti- β -galactosidase (1 : 1000). The double BrdU-NeuN immunolabeling and the immunoperoxidase BrdU labeling were performed as reported (Tang *et al.* 2009).

Immunoperoxidase BrdU labeled nuclei were counted within the subgranular zone (SGZ) of the dentate gyrus, using optical microscope Nikon TS 100 (Kingston, England), on one over eight free-floating 20- μ m sections per mouse. The number of BrdU/NeuN double labeled cells was quantified using a confocal microscope Leica TCP SP2 (Wetzlar, Germany). NeuN immunoreactivity of each BrdU cells was analyzed in the entire z-axis with a 0.5 μ m step to exclude false double labeling. One over six free-floating 25- μ m sections was analyzed per mouse, spanning the dentate gyrus.

Behavioral investigations

All the behavioral experiments were performed between 10:00 and 16:00 h, on males and/or females of both genotypes, as specified.

Elevated plus maze test

The elevated plus maze test was conducted in an apparatus consisting of a central platform (7 \times 7 cm), two open and two closed arms (30 \times 7 cm), located at a height of 55 cm above the floor, under a 50 lux illumination. Mice placed in the central platform were allowed to freely explore the maze for 5 min. Scores of mice which did make less than five entries into the open + closed arms or which did not entry into the open or closed arms were not taken into account in the statistical analyses.

Open field test

The open field test was conducted in a 100 lux illuminated sound-attenuated room. Mice were introduced in a corner of the arena (100 \times 100 \times 30 cm) and allowed to freely explore the open field for 9 min. Scores of mice that did not visit the central square were not taken into account in the statistical analyses.

Tail suspension test

Thirty minutes after i.p. administration of saline or venlafaxine, mice were suspended by the tail, using a paper adhesive tape, to a hook in a chamber of the apparatus (Idtech Bioseb ATP, Vitrolles, France). Their immobility time was mechanically and automatically recorded during a 6-min test period.

Treadmill locomotion

Motor performances of female mice were assessed according to (Antri *et al.* 2003; Lapointe *et al.* 2006). Briefly, mice were placed with all four limbs on a moving treadmill and allowed to walk freely. In order to determine the maximal speed (V_{\max}) at which mice were able to run, the speed of the treadmill belt was progressively increased until mice gave up running. The evaluation of locomotor capabilities of the animals was done by the observation of four parameters: capability to support the body weight with limbs, interlimb coordinations, quality of foot placement on the walking surface and amplitude of the locomotor movement. Motor performances were quoted on a scale using a maximal score of 22 points.

Statistical analyses

Data were subjected to factorial one-, two-, three or four-way ANOVA, with sex, genotype or treatment as between-group factors and time as within-group factor. Significant main effects were further analyzed by *post hoc* comparisons of means using Fisher's test.

The concentration of ipsapirone producing 50% reduction (IC_{50}) of DR 5-HT neuron firing was calculated by nonlinear regression using GraphPad Prism 5.0a software (GraphPad Software Inc., La Jolla, CA, USA). The means \pm SEM were compared using Student's *t*-test. For all tests, statistical significance was set at $p < 0.05$.

Results

5-HT levels and *in vivo* tryptophan hydroxylase activity

We first measured the tissue levels of 5-HT and its main metabolite 5-HIAA, as well the *in vivo* TPH2 activity in various areas of WT and STOP KO mice of both genders in equal proportion (Table 1). No significant differences between genders [5-HT: $F_{(1,68)} = 0.84$; 5-HIAA: $F_{(1,68)} = 0.02$, 5-HTP: $F_{(1,127)} = 0.09$] were noted and data for males and females were pooled.

A trend to higher levels of 5-HT and 5-HIAA was found in the brainstem containing the raphe nuclei in STOP KO vs. WT mice. In contrast, 5-HT and 5-HIAA levels were significantly lower in forebrain areas in mutant mice, except in the substantia nigra plus the ventral tegmental area where no differences were found compared to WT mice. The parallel decreases of 5-HT and 5-HIAA levels resulted in no significant modifications of their ratio in all studied areas, suggesting that the turnover of 5-HT was not altered in STOP KO vs. WT mice.

The *in vivo* TPH2 activity (estimated from 5-HTP accumulation) in STOP KO vs. WT mice was significantly higher in the brainstem, lower in the hippocampus, the striatum and the frontal cortex and not modified in the substantia nigra + the ventral tegmental area and in the nucleus accumbens.

5-HT transporter densities

The densities of the 5-HT transporter (SERT) were determined by quantification of autoradiographic [3 H]citalopram labeling in various brain areas of WT and STOP KO mice of both genders in equal proportion (Fig. 1, Table 2). Analyses of data showed no significant effect of gender [$F_{(1,348)} = 0.11$].

The relative density of SERT was markedly altered in all areas studied in STOP KO vs. WT mice. It was significantly higher by 90–120% in both the dorsal and median raphe nuclei and by 40–60% in the substantia nigra and the ventral tegmental area of mutants compared to WT mice. In contrast, SERT level was significantly less in all forebrain areas examined in mutants. The amplitude of the reduction varied from 20% to 90%, according to areas.

Table 1 5-HT and 5-HIAA levels and *in vivo* TPH2 activity in some brain areas of WT and STOP KO mice

| Area | Genotype | 5-HT | 5-HIAA | 5-HTP |
|-------------------|----------|----------------------------|----------------------------|--------------------------|
| Brainstem | WT | (6) 0.65 ± 0.07 | (6) 0.65 ± 0.06 | (6) 374 ± 15 |
| | KO | (6) 0.78 ± 0.06 +19% ns | (6) 0.80 ± 0.08 +23% ns | (6) 492 ± 29 +32%** |
| SN + VTA | WT | (6) 1.23 ± 0.09 | (6) 0.82 ± 0.08 | (12) 729 ± 67 |
| | KO | (6) 1.31 ± 0.13 +6% ns | (6) 0.88 ± 0.07 +7% ns | (12) 838 ± 82 +15% ns |
| Hippocampus | WT | (6) 0.33 ± 0.03 | (6) 0.25 ± 0.03 | (12) 214 ± 13 |
| | KO | (6) 0.17 ± 0.02 -48%** | (6) 0.16 ± 0.02 -36%* | (11) 115 ± 10 -46%*** |
| Caudate putamen | WT | (6) 0.45 ± 0.06 | (6) 0.30 ± 0.04 | (11) 226 ± 14 |
| | KO | (6) 0.28 ± 0.03 -38%* | (6) 0.20 ± 0.02 -33%* | (13) 175 ± 16 -22%* |
| Nucleus accumbens | WT | (6) 0.38 ± 0.03 | (6) 0.26 ± 0.01 | (12) 296 ± 30 |
| | KO | (6) 0.20 ± 0.03 -48%*** | (6) 0.16 ± 0.02 -39%** | (12) 262 ± 22 -12% ns |
| Frontal cortex | WT | (6) 0.42 ± 0.03 | (6) 0.18 ± 0.02 | (12) 154 ± 9 |
| | KO | (6) 0.20 ± 0.02 -51%*** | (6) 0.08 ± 0.01 -54%*** | (12) 100 ± 11 -35%*** |

5-HT and 5-HIAA levels are expressed as means ± SEM in µg/g fresh tissue. For the determination of *in vivo* TPH2 activity, mice received 100 mg/kg NSD 1015 30 min before killing. Respective basal 5-HTP levels were subtracted from 5-HTP accumulated after NSD 1015 administration. Data are expressed as means ± SEM in ng/g/30 min. The number of total mice (equal number of females and males) is indicated in parentheses. SN, substantia nigra; VTA, ventral tegmental area. Fisher's test: ns, non-significant; * $p < 0.050$; ** $p < 0.005$; *** $p < 0.001$, comparison between genotypes.

The opposite variations of SERT levels in brainstem vs. forebrain areas were confirmed by measuring [³H]citalopram specific binding to membrane preparations (Table S1).

Analysis of the variations of SERT density in various brain areas of STOP KO compared to WT mice showed that they grossly followed both rostro-caudal and dorso-ventral gradients, with the higher decrease in the retrosplenial cortex at the anteriority level of the raphe nuclei and of the substantia nigra in mutants (Table 2). A highly significant correlation [$r^2 = 0.8364$, $F_{(1,26)} = 148.3$, $p < 0.0001$] was found between SERT level decreases and 5-HT fiber length (determined according to Vertes 1991 and Vertes *et al.* 1999; Figure S1).

Density and function of the 5-HT1A autoreceptors

We quantified the densities of 5-HT1A receptors radiolabeled by [³H]WAY100635 (Fig. 1, Table 3), localized on both the serotonergic (autoreceptors) and non-serotonergic (post-synaptic receptors) somas (Verge *et al.* 1986). Analyses of data showed no significant effect of gender (equal proportion of females and males, $F_{(1,256)} = 0.39$).

In STOP KO compared to WT mice, the density of 5-HT1A receptors was significantly increased by 60–70% in the dorsal and median raphe nuclei and by 30% in the retrosplenial cortex, at the anteriority level of the substantia

nigra, whereas it was not significantly modified in all the other areas studied, except in the cingulate cortex where it decreased by 20%.

We then assessed whether the increased 5-HT1A autoreceptor labeling has consequences on the control of 5-HT neuron firing (Fig. 2). Statistical analysis revealed no significant effect of genotype on the basal firing activity of serotonergic neurons in the dorsal raphe nucleus of STOP KO compared to WT male mice (Fig. 2b). The addition of the 5-HT1A receptor agonist ipsapirone to aCSF superfusing slices resulted in a concentration-dependent inhibition of the dorsal raphe neuron firing (Fig. 2a and c). Inhibitions by ipsapirone at 30 and 60 nM were significantly higher in STOP KO than in WT mice (Fig. 2c). This larger response in mutant mice yielded a leftward displacement of the concentration-response curve and a significant 37% decrease of the IC₅₀ value of ipsapirone, that is, $35.6 ± 2.7$ nM and $22.3 ± 1.5$ nM, $p < 0.01$, in WT vs. STOP KO mice, respectively.

Serotonin soma counting and fiber density determination

Serotonergic somas of male WT and STOP KO mice were labeled by an antiserum directed against either TPH2, or 5-HT after administration of a monoamine oxidase A inhibitor to increase 5-HT tissue levels (Fig. 3 and Table 4). Seroto-

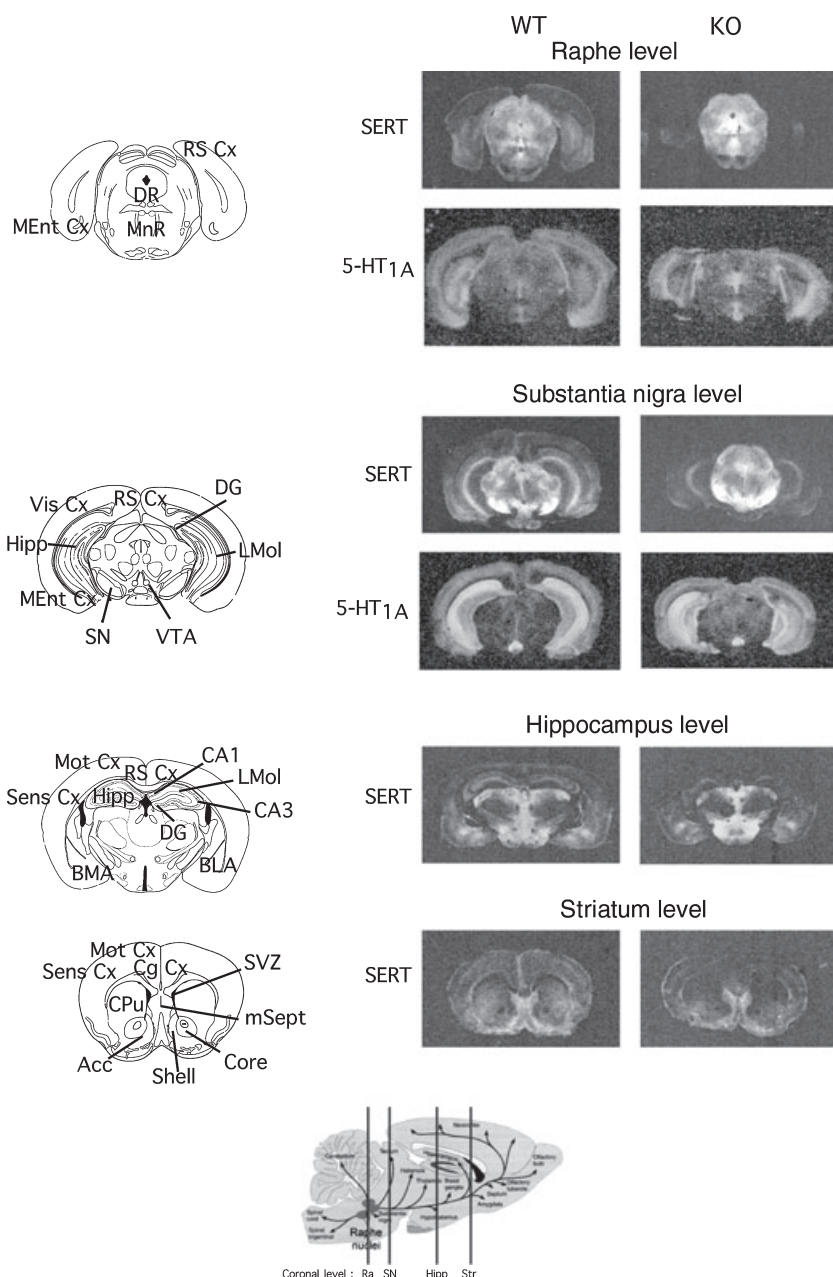


Fig. 1 Representative autoradiographic labelings of serotonin transporter (SERT) and 5-HT_{1A} receptors in brain areas of WT and STOP KO mice. Note that the labeling of SERT and 5-HT_{1A} receptors was performed on consecutive slices and, consequently, that the greatly diminished SERT labeling in the STOP KO mouse cortical areas was not because of a loss of cortical tissues. Bottom: Schematic representation of the 5-HT brain pathways ([http://www.colorado.edu/intphys/Class/IPHY3730/image/figure 6-6](http://www.colorado.edu/intphys/Class/IPHY3730/image/figure%206-6)) and of the four coronal levels studied: anterior raphe nuclei (Ra, bregma = -4.20 to -4.60), substantia nigra (SN, bregma = -2.92 to -3.88), dorsal hippocampus (Hipp, bregma = -1.06 to -1.80) and striatum (Str, bregma = 1.54 to 0.98), according to Franklin and Paxinos (1997). Acc, nucleus accumbens; BLA, basolateral amygdala; BMA, basomedial amygdala; CA1-CA3, CA1, CA3 fields of Ammon's horn in the hippocampus; Cg Cx, cingulate cortex; Core, core of the nucleus accumbens; CPu, caudate-putamen; DG, dentate gyrus of the hippocampus; DR, dorsal raphe nucleus; Hipp, hippocampus; LMol, lacunosum moleculare field of the hippocampus; MEEnt Cx, Medial entorhinal cortex; MnR, median raphe nucleus; Mot Cx, motor cortex; mSept, medial septum; RS Cx, retrosplenial cortex; Sens Cx, somatosensory cortex; Shell, shell of the nucleus accumbens; SN, substantia nigra; SVZ, subventricular zone; Vis Cx, visual cortex; VTA, ventral tegmental area.

nergic terminals were immunolabeled by a SERT antiserum in two projection areas, the dentate gyrus in the dorsal hippocampus and the cingulate cortex. Statistical analyses of data in the raphe nuclei showed a significant effect of area [$F_{(1,32)} = 500.41$, $p < 0.0001$], but no significant effect of the genotype and antiserum. As cell bodies were numbered without taking into account the intensity of the TPH2 immunostaining per soma, it is difficult to assess if the higher *in vivo* synthesis rate in the brainstem of STOP KO mice (Table 1) was because of an increased TPH2 availability and/or to change in its kinetic properties.

In contrast, analyses of data in the two terminal areas examined showed a significant effect of genotype and area on

the SERT immunolabeled serotonergic fiber density [genotype: $F_{(1,16)} = 103.81$, $p < 0.0001$; area: $F_{(1,16)} = 16.58$, $p = 0.0009$; genotype \times area: $F_{(1,16)} = 6.30$, $p = 0.0232$]. A profound decrease of SERT immunostained fibers was found in both the dentate gyrus of the anterior hippocampus (-60%) and the cingulate cortex (-66%) of STOP KO mice, in agreement with SERT autoradiographic labeling data.

Quantitative determination of neurogenesis

Neurogenesis was quantified in the adult hippocampus and subventricular zone of male mice of both genotypes (Figs 4 and S3). We first compared the progenitor cell proliferation in the SGZ of the dentate gyrus of WT and

Table 2 Densities of SERT in brain areas of WT and STOP KO mice

| Coronal level | Area | WT | KO | KO/WT (%) |
|---------------|---------|------------------|------------------|-----------|
| Raphe | RS Cx | (6) 7.3 ± 1.1 | (6) 0.60 ± 0.15 | -92*** |
| | DR | (6) 103.3 ± 20.6 | (6) 227.4 ± 17.9 | +121** |
| | MnR | (6) 106.1 ± 14.8 | (6) 201.2 ± 13.2 | +90** |
| | MEnt Cx | (6) 10.2 ± 1.3 | (6) 1.9 ± 0.4 | -82*** |
| SN | RS Cx | (7) 11.0 ± 0.8 | (6) 0.92 ± 0.15 | -92*** |
| | Vis Cx | (7) 8.4 ± 0.7 | (6) 1.4 ± 0.2 | -84*** |
| | SN | (7) 144.5 ± 11.0 | (6) 206.1 ± 8.7 | +43** |
| | VTA | (7) 114.1 ± 10.2 | (6) 181.9 ± 13.4 | +59** |
| | Hipp | (7) 26.1 ± 1.7 | (6) 12.2 ± 0.7 | -55*** |
| | DG | (7) 22.7 ± 3.2 | (6) 9.0 ± 0.8 | -61** |
| | LMol | (7) 35.4 ± 2.8 | (6) 17.1 ± 1.1 | -52*** |
| | MEnt Cx | (7) 38.4 ± 2.5 | (6) 10.4 ± 2.2 | -73*** |
| Hippocampus | RS Cx | (6) 18.9 ± 1.9 | (6) 4.6 ± 0.2 | -75*** |
| | Mot Cx | (6) 10.6 ± 1.5 | (6) 2.7 ± 0.4 | -75*** |
| | Sens Cx | (6) 11.0 ± 1.3 | (6) 3.5 ± 0.4 | -68** |
| | Hipp | (6) 18.6 ± 2.2 | (6) 12.5 ± 0.6 | -33* |
| | CA1 | (6) 16.6 ± 1.8 | (6) 9.9 ± 0.6 | -40* |
| | CA3 | (6) 23.0 ± 2.9 | (6) 12.6 ± 1.0 | -45** |
| | DG | (6) 31.3 ± 3.0 | (6) 24.4 ± 1.2 | -22* |
| | LMol | (6) 25.5 ± 1.3 | (6) 17.8 ± 1.3 | -30* |
| | BLA | (6) 72.4 ± 6.3 | (6) 45.8 ± 1.2 | -37* |
| | BMA | (6) 59.1 ± 7.3 | (6) 39.5 ± 1.5 | -33* |
| Striatum | Cg Cx | (7) 33.7 ± 2.7 | (7) 12.3 ± 1.7 | -64*** |
| | Mot Cx | (7) 19.5 ± 1.9 | (7) 9.8 ± 1.1 | -50** |
| | Sens Cx | (7) 21.6 ± 2.0 | (7) 14.1 ± 0.9 | -35* |
| | CPu | (7) 29.6 ± 2.2 | (7) 17.1 ± 1.1 | -42** |
| | SVZ | (5) 33.7 ± 3.4 | (5) 20.2 ± 2.6 | -40* |
| | N Acc | (7) 36.2 ± 2.4 | (7) 25.2 ± 1.8 | -30* |

Densities are the means ± SEM of specific [³H]citalopram autoradiographic labelings in nCi/mg. The total number of mice (quasi equal proportion of females and males) is indicated in parentheses. See Fig. 1 for the anteriority of the various coronal levels. BLA, basolateral amygdala; BMA, basomedial amygdala; CA1–CA3, CA1, CA3 fields of Ammon's horn in the hippocampus; Cg Cx, cingulate cortex; CPu, caudate-putamen; DG, dentate gyrus of the hippocampus; DR, dorsal raphe nucleus; Hipp, hippocampus; LMol, lacunosum moleculare field of the hippocampus; MEnt Cx, Medial entorhinal cortex; MnR, median raphe nucleus; Mot Cx, motor cortex; N Acc, nucleus accumbens; RS Cx, retrosplenial cortex; Sens Cx, somatosensory cortex; SN, substantia nigra; SVZ, subventricular zone; Vis Cx, visual cortex; VTA, ventral tegmental area. Fisher's test: * $p < 0.010$, ** $p < 0.001$, *** $p < 0.0001$, comparison between genotypes.

STOP KO adult mice and found a significant 28% decrease [$F_{(1,13)} = 8.47$, $p = 0.034$] in the number of BrdU positive cells in mutants (Fig. 4a). Furthermore, the number of BrdU/NeuN positive cells was significantly decreased by 53% [$F_{(1,6)} = 7.47$, $p = 0.0122$] in the granular layer of STOP KO mice (Fig. 4b). These results indicated a deficit in the number of both proliferating cells and integrated new neurons in mutants. In contrast, no significant effect of genotype was found on the number of BrdU positive cells in the subventricular zone (SVZ) and of new neurons in the granular layer of the olfactory bulb (Figure S3).

Hippocampal localization of the STOP protein

To assess the potential effect of STOP protein on neurogenesis, we characterized its expression profile in the two adult germinal zones, SGZ and SVZ. In the hippocampus, STOP immunolabeling was found mostly in dendrites and axons, but not in the cell bodies (Andrieux *et al.* 2002; Couegnas *et al.* 2007). Thus, a direct immunolabeling of STOP protein does not allow a precise identification of individual neurons expressing STOP protein. We took advantage of the knockout mouse construction where the lacZ gene was introduced under the control of the STOP promoter to establish the profile of STOP transcription in

| Coronal level | Area | WT | KO | KO/WT (%) |
|---------------|---------|------------------|------------------|-----------|
| Raphe | RS Cx | (6) 8.18 ± 0.31 | (7) 8.18 ± 0.28 | 0 |
| | DR | (6) 9.13 ± 1.07 | (7) 15.53 ± 1.02 | +70** |
| | MnR | (6) 8.77 ± 0.97 | (7) 14.12 ± 1.19 | +61* |
| | MEnt Cx | (6) 14.37 ± 0.93 | (7) 15.16 ± 0.49 | +6 ns |
| SN | RS Cx | (7) 6.18 ± 0.21 | (6) 8.16 ± 0.18 | +32** |
| | Hipp | (7) 20.57 ± 1.42 | (6) 20.00 ± 0.55 | -3 ns |
| | CA1 | (7) 29.25 ± 1.74 | (6) 26.90 ± 1.59 | -8 ns |
| | DG | (7) 12.65 ± 0.63 | (6) 13.76 ± 0.76 | +9 ns |
| | LMol | (7) 35.95 ± 3.59 | (6) 30.05 ± 1.40 | -15 ns |
| | MEnt Cx | (6) 9.04 ± 0.54 | (6) 9.28 ± 0.34 | +3 ns |
| Hippocampus | RS Cx | (6) 7.15 ± 0.35 | (7) 7.00 ± 0.41 | -2 ns |
| | Hipp | (7) 24.48 ± 0.82 | (8) 23.14 ± 1.11 | -5 ns |
| | CA1 | (6) 36.41 ± 0.79 | (6) 36.07 ± 1.18 | -1 ns |
| | CA3 | (6) 14.84 ± 0.69 | (6) 12.64 ± 0.39 | -15 ns |
| | LMol | (6) 36.54 ± 1.28 | (6) 37.73 ± 0.59 | +3 ns |
| | BLA | (6) 15.16 ± 0.83 | (7) 15.34 ± 0.78 | -1 ns |
| | BMA | (6) 14.42 ± 1.35 | (7) 12.17 ± 1.44 | -16 ns |
| Striatum | Cg Cx | (7) 10.00 ± 0.48 | (8) 8.22 ± 0.24 | -18* |
| | lSept | (7) 24.30 ± 1.30 | (6) 24.36 ± 0.72 | 0 |
| | mSept | (7) 28.44 ± 1.13 | (6) 27.18 ± 0.0 | -4 ns |

Table 3 Density of 5-HT_{1A} receptor in brain of WT and STOP KO mice

Densities are the means ± SEM of specific autoradiographic [³H]WAY 100635 labelings in nCi/mg. The total number of mice (quasi equal proportion of females and males) is indicated in parentheses. See Fig. 1 for the anteriority of the various coronal levels. BLA, basolateral amygdala; BMA, basomedial amygdala; CA1–CA3, CA1, CA3 fields of Ammon's horn in the hippocampus; Cg Cx, cingulate cortex; DG, dentate gyrus of the hippocampus; DR, dorsal raphe nucleus; Hipp, hippocampus; LMol, lacunosum moleculare field of the hippocampus; lSept, lateral septum; MEnt Cx, Medial entorhinal cortex; MnR, median raphe nucleus; mSept, medial septum; RS Cx, retrosplenial cortex. Fisher's test: ns, non-significant, **p* < 0.010, ***p* < 0.001, comparison between genotypes.

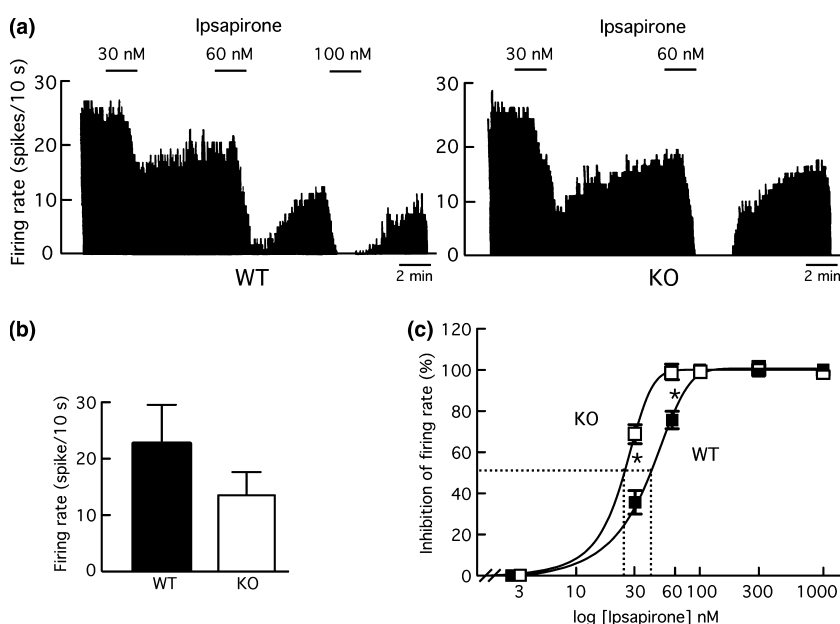


Fig. 2 Electrophysiological effect of the 5-HT_{1A} autoreceptor agonist ipsapirone in the dorsal raphe of WT and STOP KO male mice. (a) Integrated firing rate histograms (in spikes/10 s), with or without ipsapirone at increasing concentrations. (b) Spontaneous firing rate in WT and STOP KO mice. (c) Concentration-dependent inhibition by ipsapirone of the firing of 5-HT neurons. Inhibitions (means ± SEM of three WT and four KO) are expressed as % of basal firing. The dotted lines illustrate the determination of the IC₅₀ values. **p* < 0.010 by the Fisher's test.

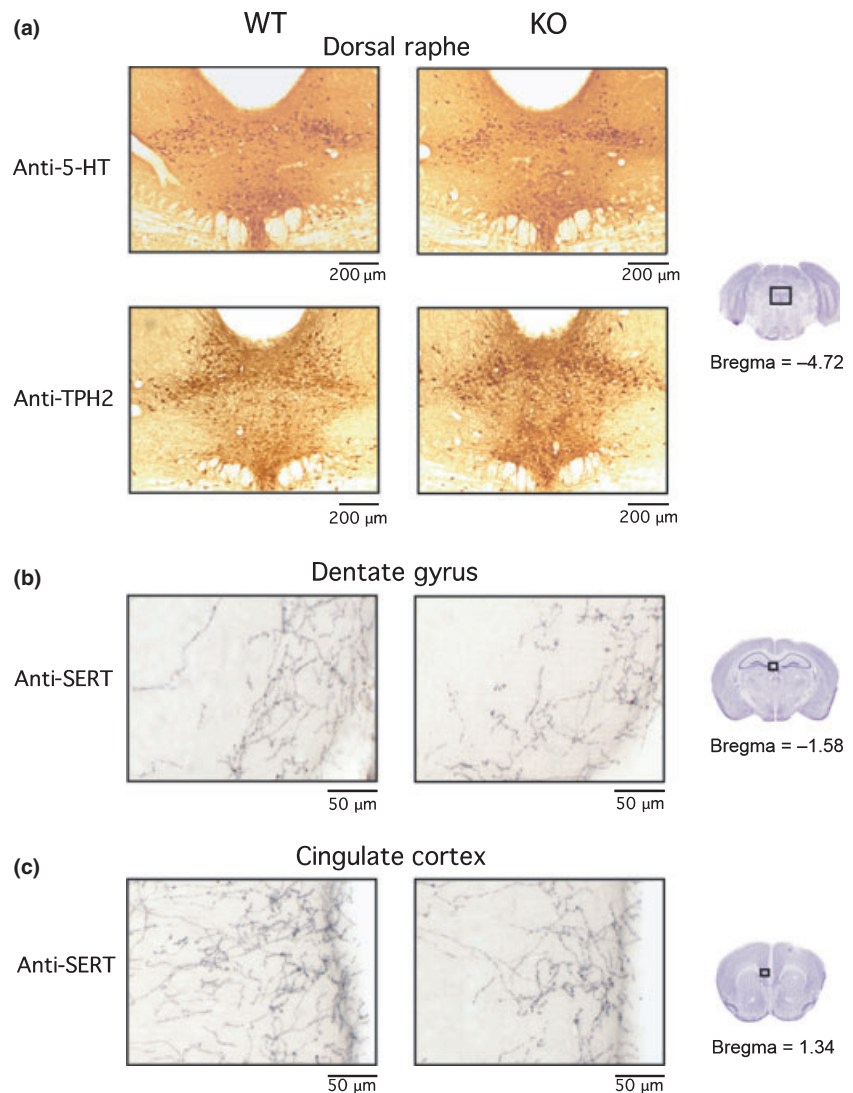


Fig. 3 Determination of the number of 5-HT somas and of the density of 5-HT terminals in WT vs. STOP KO male mice. Serotonergic somas at the level of the dorsal and median raphe nuclei were immunolabeled by antiserum against 5-HT or TPH2. Terminals at the level of dentate gyrus of the hippocampus and of cingulate cortex were immunolabeled with an antiserum against SERT.

Table 4 5-HT soma number and terminal density in brain areas of WT and STOP KO mice

| Area | Antibody | WT | KO | KO/WT (%) |
|-------------------------------------|-----------|-------------------|-------------------|-----------|
| Number of somas | | | | |
| Dorsal raphe | Anti-5-HT | (5) 372 ± 19 | (5) 376 ± 21 | +1 ns |
| | Anti-TPH2 | (5) 388 ± 24 | (5) 375 ± 25 | -3 ns |
| Median raphe | Anti-5-HT | (5) 119 ± 4 | (5) 120 ± 3 | +1 ns |
| | Anti-TPH2 | (5) 123 ± 7 | (5) 132 ± 5 | +7 ns |
| Fiber density (μm/μm ²) | | | | |
| Dentate gyrus | Anti-SERT | (5) 0.068 ± 0.003 | (5) 0.027 ± 0.004 | -60* |
| Cingulate cortex | Anti-SERT | (5) 0.104 ± 0.006 | (5) 0.035 ± 0.008 | -66* |

Data are the means ± SEM. The number of male mice is indicated in parentheses. *Post hoc* Fisher's test: ns, non-significant, * $p < 0.001$, comparison between genotypes.

the adult germinal zones, by β -galactosidase immunostaining present in the cytoplasmic/nuclear compartment (Couegnas *et al.* 2007).

Expression of β -galactosidase in the granular layer of the dentate gyrus of male heterozygous mice appeared mostly

in cells co-expressing the mature neuronal marker NeuN (Fig. 4c-i,ii) and in cells positive for DCX located in the molecular layer (probably corresponding to granule cells starting integrating process). In contrast, neither immature migrating neurons located in the SGZ (Fig. 4c-iii), nor

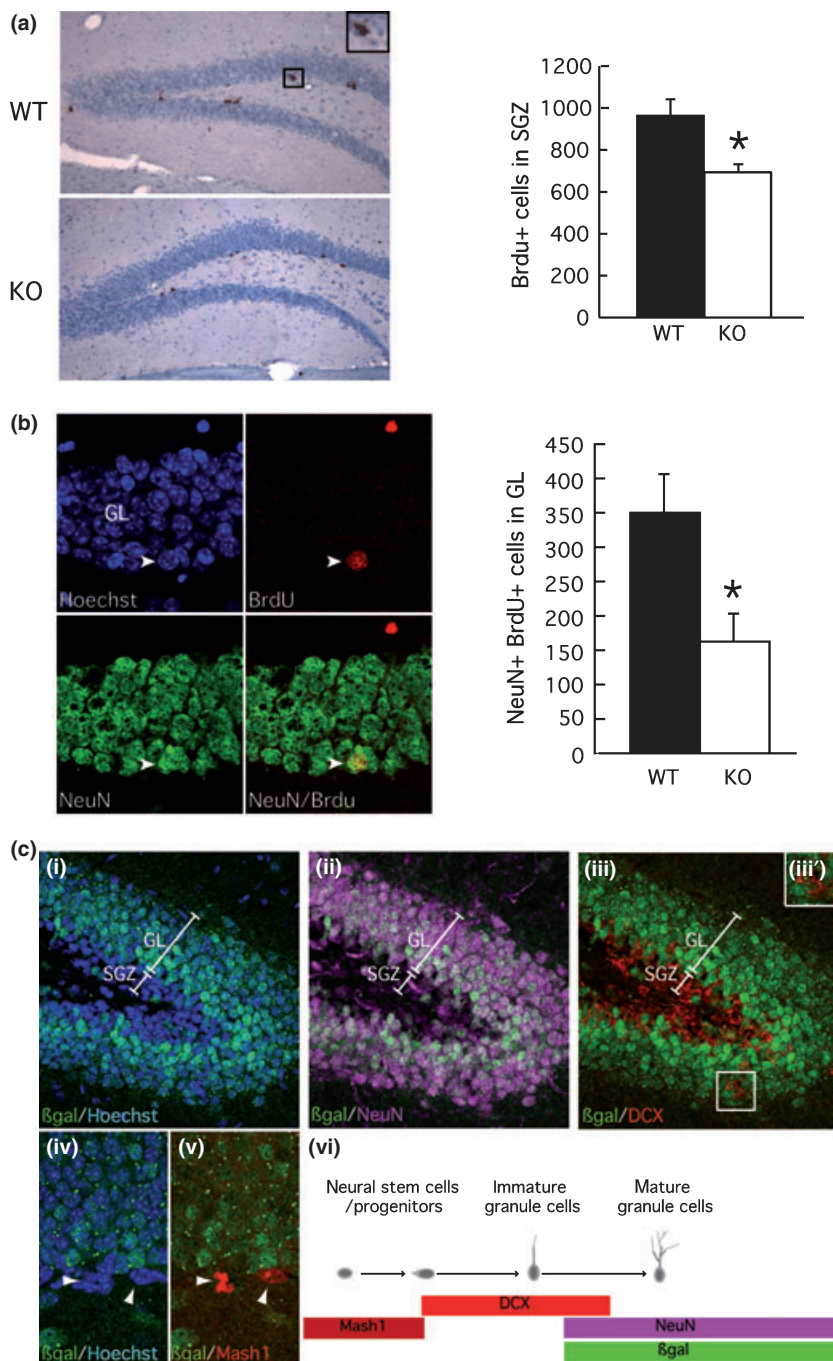


Fig. 4 Neurogenesis in the hippocampus of adult WT and STOP KO male mice. (a) Left: representative photograph of BrdU peroxidase immunolabeled cells in the dentate gyrus of WT and STOP KO mice. Inset shows a cluster of BrdU positive cells. Right: number (means ± SEM of nine WT and six KO mice) of BrdU-positive cells in the subgranular zone (SGZ) of the dentate gyrus (coronal level: Bregma -1.22 to -2.70). (b) Left: confocal imaging reveals that BrdU positive (red) newborn cells in the granular layer (GL) of dentate gyrus differentiate into mature NeuN (green) neurons (arrowhead). Right: number (means ± SEM of four WT and four KO mice) of double BrdU- and NeuN-positive cells in the granular layer (GL) of the dentate gyrus. (c) Promoter STOP activity starts with granule cells differentiation. A representative coronal brain section from heterozygous STOP mouse triple labeled for (i) β -galactosidase (STOP promoter), (ii) NeuN (mature neurons), (iii) doublecortin (DCX, immature granule cells), or double immunolabeled for (iv–v) β -galactosidase and Mash1 (progenitors). In (iii), the inset shows that only DCX positive cells within the GL expressed β -galactosidase. In (vi), schematic representation of markers expressed during the granular cell development. Means ± SEM; Fisher's test: * $p < 0.05$.

Mash1 positive cells, corresponding mainly to proliferating cells (Parras *et al.* 2004), expressed β -galactosidase (Fig. 4c-iv,v). These data showed that the STOP reporter gene was absent in both progenitor and immature granule cells and started to be expressed in mature granule cells (Fig. 4c-vi).

Finally, we did not detect STOP expression in progenitors or neuroblasts within the SVZ (not shown) and, surprisingly, we did not detect STOP expression in granular and periglomerular neurons within the olfactory bulb (Figure S3).

Anxiety- and depression-related behaviors of WT and STOP KO mice

Using validated paradigms, we determined the anxiety- and depression-like status of WT and STOP KO mice of both genders in approximately equal proportion.

In the elevated plus-maze test (Fig. 5a), statistical analyses showed no effect of gender and genotype on the total time spent [$F_{(1,45)} = 0.53$ and $F_{(1,45)} = 0.23$, respectively] and the number of entries [$F_{(1,45)} = 0.14$ and $F_{(1,45)} = 3.33$, respectively] in the open + closed arms. However, significant

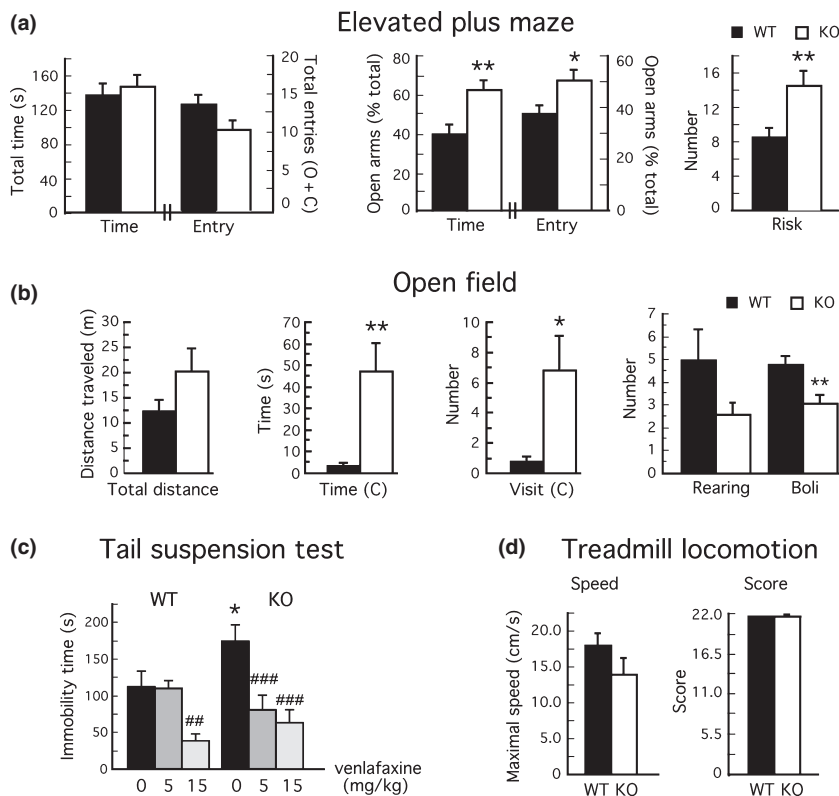


Fig. 5 Anxiety- and depression-status of WT and STOP KO mice. (a) Elevated plus maze test. Mice were tested for their time spent and number of entries in the open and closed arms and for their numbers of head-dipping (risk). Values are the means \pm SEM for 11 females/15 males WT and 11 females/12 males STOP KO. Analyses showed significant effects of gender and genotype on the percentage of time spent in open arms [$F_{(1,45)} = 12.20$, $p = 0.0011$, $F_{(1,45)} = 10.02$, $p = 0.0028$, respectively], on the percentage of entries into the open arms [$F_{(1,45)} = 13.91$, $p = 0.0005$, $F_{(1,45)} = 6.78$, $p = 0.0124$, respectively] and on the risk taking [$F_{(1,45)} = 8.31$, $p = 0.0060$, $F_{(1,45)} = 11.03$, $p = 0.0018$, respectively]. (b) Open field test. Mice were tested for their distance traveled, their time spent and number of visits in the central square, as well as for their numbers of rearings and boli. Values are the means \pm SEM for 10 females/12 males WT and 12 females/11

males STOP KO. The effect of genotype was significant on the time spent in the center [$F_{(1,41)} = 9.85$, $p = 0.0031$], on the number of visits in the central square [$F_{(1,41)} = 6.58$, $p = 0.014$] and on the number of boli [$F_{(1,41)} = 10.57$, $p = 0.0023$]. (c) Tail suspension test. Thirty minutes after administration of saline or venlafaxine, mice were tested for their immobility time. Means \pm SEM for four to six mice per gender, per genotype and per treatment. The effect of treatment and of the interaction between treatment and genotype were significant [treatment: $F_{(2,50)} = 11.16$, $p < 0.0001$; treatment \times genotype: $F_{(2,50)} = 3.85$, $p = 0.0453$]. (d) Comparison of locomotor performances of WT and STOP mice in the running treadmill. Means \pm SEM for six WT and six STOP KO females. *Post hoc* Fisher's test: * $p < 0.05$, ** $p < 0.010$, comparison between genotypes; ### $p < 0.010$; #### $p < 0.001$, comparison between treatment.

effects of gender and genotype (but not of gender \times genotype) were seen on the percentage of time spent in the open arms, on the percentage of entries into the open arms and on the risk taking (see legend to Fig. 5a).

The time spent by STOP KO mice and their number of entries in the open arms were significantly increased by 1.60- (females: 1.43, males: 1.70) and 1.35-fold (females: 1.35, males: 1.29) compared to WT mice, respectively. Furthermore, mutant mice displayed a 70% (females: 102%, males: 30%) increase in the risk-taking (number of head-dipping).

In the open field test (Fig. 5b), analyses of data showed no significant effect of gender on all parameters tested [$F_{(1,41)} = 0.10$ –3.06] and no effect of genotype on the total length traveled [$F_{(1,41)} = 2.43$] and on the rearing [$F_{(1,41)} =$

2.39]. In contrast, the effect of genotype (but not of gender \times genotype) was significant on the time spent in the center, on the number of visits in the central square and on the number of boli (see legend to Fig. 5b).

The locomotor activity was 1.6-fold higher (although non-significantly) in STOP KO than in WT mice, in agreement with previous observations (Brun *et al.* 2005; Bouvrais-Veret *et al.* 2007, 2008). In addition, the time spent and the number of entries in the central square by mutant mice were 14-fold and 9-fold higher than those of WT mice, respectively. In contrast, the number of boli was significantly less (–37%) in STOP KO mice.

The depression/helplessness-status of WT and STOP KO mice was assessed in the tail suspension test. As

preliminary data also showed decreased levels of norepinephrine in forebrain areas of STOP KO mice (not shown), venlafaxine, a mixed inhibitor of both 5-HT and norepinephrine reuptake, was used in these experiments (Fig. 5c). Analysis of data showed no significant effect of gender or gender \times genotype [$F_{(1,50)} = 3.23$ and 0.07 , respectively], but a significant effect of treatment and of the interaction between treatment and genotype were seen (see legend to Fig. 5c).

The immobility time of saline-treated STOP KO mice was significantly increased by 55% ($p = 0.0151$) as compared to saline-treated WT mice. Moreover, venlafaxine (5 mg/kg) significantly reduced ($-54%$, $p = 0.0005$), the immobility time in mutant mice, but was ineffective in WT mice.

The numerous falls of STOP KO mice from the open arms in the elevated plus-maze and the involvement of serotonin transmission in the locomotor function (Antri *et al.* 2003) prompted us to evaluate the quality of locomotor movements in these mutants compared to WT mice (Fig. 5d), using the running treadmill locomotion test. Statistical analysis of performance of WT and STOP KO females showed no significant effect of genotype on the maximal speed and on the motor performance, suggesting that STOP KO mice had neither gross equilibrium deficit nor locomotor movement impairment.

Discussion

Our data showed that the deletion of the STOP protein triggered dramatic imbalance of the serotonin neurotransmission in cell body vs. projection areas, with accumulation of some key-proteins in the somas and decreased levels of these proteins in terminals. The significant correlation between SERT density decreases and 5-HT fiber length suggested that the STOP deletion impaired either the axonal transport of the SERT protein or the differentiation of 5-HT fibers. These dysfunctions of the 5-HT system were probably associated with altered performance of STOP KO mice in tests assessing anxiety- and depression-like behaviors. In addition, adult hippocampal neurogenesis was found to be markedly less in STOP KO compared to WT mice, potentially because of STOP deletion *per se* and 5-HT neurotransmission peculiarities.

Accumulation of some markers at the level of the serotonergic cell bodies

At the level of the serotonergic somas in STOP KO mice, our data showed moderate increase in tissue 5-HT levels and *in vivo* synthesis rate and sustained increases in the serotonin transporter SERT and the 5-HT_{1A} autoreceptor densities. However, we did not detect significant differences in the number of 5-HT somas in anterior raphe nuclei between mutant and WT mice. These results

suggest that the STOP deletion induced an accumulation of 5-HT and serotonergic proteins in the cell bodies, rather than a higher density of serotonergic somas. The increased density of the 5-HT_{1A} autoreceptors in STOP KO mice was functional, as their agonist ipsapirone was more efficacious to inhibit 5-HT neuron firing in the dorsal raphe nucleus of mutant compared to WT mice. Such increases in both the density and sensitivity of 5-HT_{1A} autoreceptors in mutant mice might be adaptive changes compensating for a decreased *in vivo* concentration of extracellular 5-HT. Indeed, SERT over-expression in the raphe nuclei, which caused a marked increase in 5-HT reuptake, should down-regulate extracellular 5-HT levels in these mutants.

Decreased levels of some 5-HT proteins in the terminal areas

In contrast to that observed at the 5-HT soma level, STOP KO mice exhibited in all terminal regions, except in dopaminergic cell body areas, marked decreases in tissue 5-HT levels and *in vivo* synthesis rate, associated with a 30–90% decrease of SERT density, with no modification of post-synaptic 5-HT_{1A} receptor density. Such a decrease in endogenous 5-HT level has been reported in brain of mice lacking SERT (Bengel *et al.* 1998). The amplitude of SERT decreases followed rostro-caudal and dorso-ventral gradients, corresponding approximately to fiber lengths of 5-HT widespread projections in forebrain areas (Azmitia and Segal 1978; Vertes 1991; Vertes *et al.* 1999). Interestingly, immunostaining of 5-HT terminals revealed drastic decreases of SERT positive fibers in both the anterior dentate gyrus and the cingulate cortex of STOP KO mice. Whether these decreases were because of a reduced SERT density per terminal and/or a reduced number of 5-HTergic terminals will be further explored. In the substantia nigra and the ventral tegmental area, two dopaminergic cell body areas highly innervated by 5-HT terminals, the imbalance of 5-HT neurotransmission was intermediate between 5-HT somas and terminals. Among the 5-HT parameters tested, only the SERT density was significantly increased in mutant mice. Whether this intermediate situation was selective for these particular brain areas and/or was because of shorter 5-HTergic afferences is a question to be addressed in further investigations.

Why does deletion of the STOP protein affect more selectively the 5-HT neurotransmission?

Most of the data obtained in our study support the idea that the traffic of SERT (and perhaps of TPH2) was impaired in the absence of the STOP protein. As both 5-HT_{1A} auto- and post-synaptic receptors are exclusively located in the somatodendritic compartment (Verge *et al.* 1986; Carrel *et al.* 2008), their increased density in the two raphe nuclei could be because of increased synthesis and/or decreased

degradation rather than to their accumulation via a defective axonal transport. Moreover, the dramatic alterations of the 5-HT markers in all the studied areas of STOP KO mice contrasted with the restricted changes of the dopaminergic (Brun *et al.* 2005; Bouvrais-Veret *et al.* 2008), glutamatergic (Andrieux *et al.* 2002; Eastwood *et al.* 2007; Brenner *et al.* 2007 and our study in Appendix S1, Fig. S2) and nicotinic (Bouvrais-Veret *et al.* 2007) neurotransmissions. One can ask if the major impact of the STOP protein deletion on the serotonergic transmission could be because of the trophic role of serotonin and/or to its precocious appearance during brain ontogenesis. Among cerebral monoamines, serotonin is the neurotransmitter having the largest developmental impact on cell division, neuronal migration, cell differentiation and synaptogenesis. Furthermore, serotonergic neurons are among the earliest neurons to be generated (at around E12, Gaspar *et al.* 2003). In addition, SERT has been shown to be transiently expressed in some brain areas (including cortex, hippocampus and thalamus) during embryonic and early postnatal development (Narboux-Neme *et al.* 2008). Further investigations will have to be undertaken as, for example, the quantification of SERT levels in STOP KO mice during embryonic stages, before and after the STOP isoform appearance (at around E16, Baratier *et al.* 2006). Finally, the high variations of the density of SERT were probably in line with its implication in neuropsychiatric phenotype (Caspi *et al.* 2003; Ozaki *et al.* 2003).

The decreased hippocampal neurogenesis is rather because of the STOP protein deletion

Altered performance of STOP KO mice in some cognitive tests (Bouvrais-Veret *et al.* 2007; Powell *et al.* 2007; Begou *et al.* 2008; Delotterie *et al.* 2009) and the relationships between 5-HT neurotransmission, mechanisms of antidepressant action and hippocampal neurogenesis (David *et al.* 2009; Dranovsky and Hen 2006, but see Eisch *et al.* 2008) led us to investigate cell proliferation and differentiation in the hippocampus of these mutants. Our data showed that cell proliferation and neurogenesis were altered in this brain area but not in the SVZ of STOP KO mice. Because 5-HT-related parameters were similarly altered in all forebrain areas, this regional difference suggests that 5-HT dysfunction was most probably not fully responsible for the neurogenesis deficit in the hippocampus of STOP KO mice and/or that SERT may not be a reliable marker of 5-HT terminals in mutant mice. However, the strong correlation at the hippocampal level between STOP protein expression in WT mice and the deficit in neurogenesis in STOP KO mice suggested that STOP could be a key protein for the differentiation and/or the integration of newborn neurons in the pre-existing hippocampal network. Interestingly, such a direct effect on cell differentiation and/or integration has already been demonstrated for DISC1, another microtubule-related protein (Duan *et al.* 2007).

The anxiety- and depression-related behaviors are profoundly altered in STOP KO mice

Our behavioral studies showed that STOP KO mice were less anxious and probably more depressed (to be confirmed by other helplessness tests) than their WT littermates. Whether these behavioral alterations were the consequence of an imbalance of the serotonergic neurotransmission is an interesting question to be addressed. Indeed, the precise role of 5-HT tone in the control of emotional process is still a matter of debate as 5-HT depletion in rodents produces differential effects on their anxiety- and depression-like status (Lucki 1998). It has been reported that serotonin depletion or SERT surexpression is anxiolytic in mice (Jennings *et al.* 2006; Bechtholt *et al.* 2007) and, conversely, that the knockout of the 5-HT_{1A} receptor increases the anxiety-like status of mice (review of Leonardo and Hen 2006). On the other hand, mice lacking the SERT gene exhibit increased anxiety and depression-like behaviors (review of Murphy and Lesch 2008). In this study, we have not characterized potential alterations of the GABAergic neurotransmission and we cannot hypothesize if the decreased anxiety of STOP KO mice was underlain by GABAergic and/or serotonergic systems. Interestingly, STOP KO mice were hypersensitive to the acute effect of the antidepressant venlafaxine in the tail suspension test, suggesting a lesser competition between venlafaxine and the extracellular 5-HT level for binding to SERT and/or norepinephrine binding onto its transporter. Finally, further *in vivo* microdialysis studies will be undertaken to determine whether such a serotonergic imbalance in mutant mice was translated into hyper- or hyposerotonergia at the level of somas and/or terminals.

Conclusion

Altogether, our data show that (i) the deletion of the microtubule-associated protein STOP alters dramatically the serotonergic network in agreement with previous data on the interactions between MAPs and the serotonin neurotransmission (Bianchi *et al.* 2005), (ii) STOP is a key protein for the differentiation and/or the integration of newborn neurons in mouse adult hippocampus and (iii) STOP deletion triggers serotonergic disconnectivity, thereby providing further etiological hypothesis for psychiatric disorders such as depression and schizophrenia. Very interestingly, the fact that the microtubule stabilizer, epothilone D, can alleviate some deficits of STOP KO mice (Andrieux *et al.* 2006) may support the idea that innovative treatments of psychiatric diseases can target microtubules.

Acknowledgements

We are grateful to Dominique Divers for genotyping, Naïma Hanoun and Françoise Saurini for HPLC experiments, Jean-

François Bernard for immunostaining of 5-HT-related proteins and Caroline Bouvrais-Veret for preliminary data. This study was supported by grants from INSERM and CEE (NewMood Program LSHM-CT-2003-503474). Vincent Fournet and Marion Jany are the recipients of fellowships from the MENESR (Paris, France). The authors reported no biomedical financial interests or potential conflicts of interest.

Supporting information

Additional Supporting information may be found in the online version of this article:

Appendix S1. Supplementary Materials and Methods.

Figure S1. Correlation between the decrease of SERT level in various areas of STOP KO mice and the 5-HT fiber length.

Figure S2. Relative density of the three vesicular glutamate transporters (VGLUTs) in various brain areas of STOP KO mice.

Figure S3. Neurogenesis in the subventricular zone (SVZ) of WT and STOP KO mice.

Table S1. [³H]-Citalopram binding level on membranes from various brain areas of WT and STOP KO mice.

As a service to our authors and readers, this journal provides supporting information supplied by the authors. Such materials are peer-reviewed and may be re-organized for online delivery, but are not copy-edited or typeset. Technical support issues arising from supporting information (other than missing files) should be addressed to the authors.

References

- Aguezzoul M., Andrieux A. and Denarier E. (2003) Overlap of promoter and coding sequences in the mouse STOP gene (Mtap6). *Genomics* **81**, 623–627.
- Andrieux A., Salin P. A., Vernet M. *et al.* (2002) The suppression of brain cold-stable microtubules in mice induces synaptic defects associated with neuroleptic-sensitive behavioral disorders. *Genes Dev.* **16**, 2350–2364.
- Andrieux A., Salin P., Schweitzer A. *et al.* (2006) Microtubule stabilizer ameliorates synaptic function and behavior in a mouse model for schizophrenia. *Biol. Psychiatry* **60**, 1224–1230.
- Antri M., Mouffle C., Orsal D. and Barthe J. Y. (2003) 5-HT_{1A} receptors are involved in short- and long-term processes responsible for 5-HT-induced locomotor function recovery in chronic spinal rat. *Eur. J. Neurosci.* **18**, 1963–1972.
- Azmitia E. C. and Segal M. (1978) An autoradiographic analysis of the differential ascending projections of the dorsal and median raphe nuclei in the rat. *J. Comp. Neurol.* **179**, 641–667.
- Baratier J., Peris L., Brocard J. *et al.* (2006) Phosphorylation of microtubule-associated protein STOP by calmodulin kinase II. *J. Biol. Chem.* **281**, 19561–19569.
- Bechtholt A. J., Hill T. E. and Lucki I. (2007) Anxiolytic effect of serotonin depletion in the novelty-induced hypophagia test. *Psychopharmacology (Berl)* **190**, 531–540.
- Begou M., Brun P., Bertrand J. B., Job D., Schweitzer A., D'Amato T., Saoud M., Andrieux A. and Suaud-Chagny M. F. (2007) Post-pubertal emergence of alterations in locomotor activity in stop null mice. *Synapse* **61**, 689–697.
- Begou M., Volle J., Bertrand J. B. *et al.* (2008) The stop null mice model for schizophrenia displays [corrected] cognitive and social deficits partly alleviated by neuroleptics. *Neuroscience* **157**, 29–39.
- Bengel D., Murphy D. L., Andrews A. M., Wichems C. H., Feltner D., Heils A., Mossner R., Westphal H. and Lesch K.-P. (1998) Altered brain serotonin homeostasis and locomotor insensitivity to 3,4-methylenedioxyamphetamine (“ecstasy”) in serotonin transporter-deficient mice. *Mol. Pharmacol.* **53**, 649–655.
- Bernard J. F., Netzer F., Gau R., Hamon M., Laguzzi R. and Sevoz-Couche C. (2008) Critical role of B3 serotonergic cells in baroreflex inhibition during the defense reaction triggered by dorsal periaqueductal gray stimulation. *J. Comp. Neurol.* **506**, 108–121.
- Bianchi M., Hagan J. J. and Heidebreder C. A. (2005) Neuronal plasticity, stress and depression: involvement of the cytoskeletal microtubular system? *Curr. Drug Targets CNS Neurol. Disord.* **4**, 597–611.
- Bianchi M., Shah A. J., Fone K. C., Atkins A. R., Dawson L. A., Heidebreder C. A., Hows M. E., Hagan J. J. and Marsden C. A. (2009) Fluoxetine administration modulates the cytoskeletal microtubular system in the rat hippocampus. *Synapse* **63**, 359–364.
- Bosc C., Cronk J. D., Pirolet F., Watterson D. M., Haiech J., Job D. and Margolis R. L. (1996) Cloning, expression, and properties of the microtubule-stabilizing protein STOP. *Proc. Natl Acad. Sci. USA* **93**, 2125–2130.
- Bouvrais-Veret C., Weiss S., Andrieux A., Schweitzer A., McIntosh J. M., Job D., Giros B. and Martres M. P. (2007) Sustained increase of alpha7 nicotinic receptors and choline-induced improvement of learning deficit in STOP knock-out mice. *Neuropharmacology* **52**, 1691–1700.
- Bouvrais-Veret C., Weiss S., Hanoun N., Andrieux A., Schweitzer A., Job D., Hamon M., Giros B. and Martres M. P. (2008) Microtubule-associated STOP protein deletion triggers restricted changes in dopaminergic neurotransmission. *J. Neurochem.* **104**, 745–756.
- Brenner E., Sonnewald U., Schweitzer A., Andrieux A. and Nehlig A. (2007) Hypoglutamatergic activity in the STOP knockout mouse: a potential model for chronic untreated schizophrenia. *J. Neurosci. Res.* **85**, 3487–3493.
- Brun P., Begou M., Andrieux A. *et al.* (2005) Dopaminergic transmission in STOP null mice. *J. Neurochem.* **94**, 63–73.
- Camargo L. M., Collura V., Rain J. C., Mizuguchi K., Hermjakob H., Kerrien S., Bonnert T. P., Whiting P. J. and Brandon N. J. (2007) Disrupted in Schizophrenia 1 Interactome: evidence for the close connectivity of risk genes and a potential synaptic basis for schizophrenia. *Mol. Psychiatry* **12**, 74–86.
- Carrel D., Masson J., Al Awabdh S., Capra C. B., Lenkei Z., Hamon M., Emerit M. B. and Darmon M. (2008) Targeting of the 5-HT_{1A} serotonin receptor to neuronal dendrites is mediated by YiflB. *J. Neurosci.* **28**, 8063–8073.
- Caspi A., Sugden K., Moffitt T. E. *et al.* (2003) Influence of life stress on depression: moderation by a polymorphism in the 5-HTT gene. *Science* **301**, 386–389.
- Clapcote S. J., Lipina T. V., Millar J. K. *et al.* (2007) Behavioral phenotypes of Disc1 missense mutations in mice. *Neuron* **54**, 387–402.
- Cornea-Hébert V., Watkins K. C., Roth B. L., Kroeze W. K., Gaudreau P., Leclerc N. and Descarries L. (2002) Similar ultrastructural distribution of the 5-HT_{2A} serotonin receptor and microtubule-associated protein MAP1A in cortical dendrites of adult rat. *Neuroscience* **113**, 23–35.
- Cornea-Hébert V., Riad M., Wu C., Singh S. K. and Descarries L. (1999) Cellular and subcellular distribution of the serotonin 5-HT_{2A} receptor in the central nervous system of adult rat. *J. Comp. Neurol.* **409**, 187–209.
- Couegnas A., Schweitzer A., Andrieux A., Ghandour M. S. and Boehm N. (2007) Expression pattern of STOP lacZ reporter gene in adult and developing mouse brain. *J. Neurosci. Res.* **85**, 1515–1527.

- Craddock N. and Forty L. (2006) Genetics of affective (mood) disorders. *Eur. J. Hum. Genet.* **14**, 660–668.
- David D. J., Samuels B. A., Rainer Q. *et al.* (2009) Neurogenesis-dependent and -independent effects of fluoxetine in an animal model of anxiety/depression. *Neuron* **62**, 479–493.
- Delotterie D., Ruiz G., Brocard J., Schweitzer A., Roucard C., Roche Y., Suaud-Chagny M. F., Bressand K. and Andrieux A. (2009) Chronic administration of atypical antipsychotics improves behavioral and synaptic defects of STOP null mice. *Psychopharmacology (Berl)*, **208**, 131–141.
- Denarier E., Aguezoul M., Jolly C., Vourc'h C., Roure A., Andrieux A., Bosc C. and Job D. (1998) Genomic structure and chromosomal mapping of the mouse STOP gene (Mtap6). *Biochem. Biophys. Res. Commun.* **243**, 791–796.
- Desbonnet L., Waddington J. L. and Tuathaigh C. M. (2009) Mice mutant for genes associated with schizophrenia: common phenotype or distinct endophenotypes? *Behav. Brain Res.* **204**, 258–273.
- Dranovsky A. and Hen R. (2006) Hippocampal neurogenesis: regulation by stress and antidepressants. *Biol. Psychiatry* **59**, 1136–1143.
- Duan X., Chang J. H., Ge S. *et al.* (2007) Disrupted-In-Schizophrenia 1 regulates integration of newly generated neurons in the adult brain. *Cell* **130**, 1146–1158.
- Eastwood S. L., Lyon L., George L., Andrieux A., Job D. and Harrison P. J. (2007) Altered expression of synaptic protein mRNAs in STOP (MAP6) mutant mice. *J. Psychopharmacol.* **21**, 635–644.
- Eisch A. J., Cameron H. A., Encinas J. M., Meltzer L. A., Ming G. L. and Overstreet-Wadiche L. S. (2008) Adult neurogenesis, mental health, and mental illness: hope or hype? *J. Neurosci.* **28**, 11785–11791.
- Fabre V., Beaufour C., Evrard A. *et al.* (2000a) Altered expression and functions of serotonin 5-HT_{1A} and 5-HT_{1B} receptors in knock-out mice lacking the 5-HT transporter. *Eur. J. Neurosci.* **12**, 2299–2310.
- Fabre V., Boutrel B., Hanoun N., Lanfumey L., Fattaccini C. M., Demeneix B., Adrien J., Hamon M. and Martres M. P. (2000b) Homeostatic regulation of serotonergic function by the serotonin transporter as revealed by nonviral gene transfer. *J. Neurosci.* **20**, 5065–5075.
- Fradley R. L., O'Meara G. F., Newman R. J., Andrieux A., Job D. and Reynolds D. S. (2005) STOP knockout and NMDA NR1 hypomorphic mice exhibit deficits in sensorimotor gating. *Behav. Brain Res.* **163**, 257–264.
- Frankle W. G., Lerma J. and Laruelle M. (2003) The synaptic hypothesis of schizophrenia. *Neuron* **39**, 205–216.
- Franklin K. B. and Paxinos G. (1997) *The Mouse Brain in Stereotaxic Coordinates*. Academic Press, Inc., San Diego, CA, USA.
- Galiano M. R., Bosc C., Schweitzer A., Andrieux A., Job D. and Hallak M. E. (2004) Astrocytes and oligodendrocytes express different STOP protein isoforms. *J. Neurosci. Res.* **78**, 329–337.
- Gaspar P., Cases O. and Maroteaux L. (2003) The developmental role of serotonin: news from mouse molecular genetics. *Nat. Rev. Neurosci.* **4**, 1002–1012.
- Gottesman I. I., Laursen T. M., Bertelsen A. and Mortensen P. B. (2010) Severe mental disorders in offspring with 2 psychiatrically ill parents. *Arch. Gen. Psychiatry* **67**, 252–257.
- Guillaud L., Bosc C., Fourest-Lieuvin A., Denarier E., Pirollet F., Lafanechere L. and Job D. (1998) STOP proteins are responsible for the high degree of microtubule stabilization observed in neuronal cells. *J. Cell Biol.* **142**, 167–179.
- Hanaya R., Koning E., Ferrandon A., Schweitzer A., Andrieux A. and Nehlig A. (2008) Deletion of the STOP gene, a microtubule stabilizing factor, leads only to discrete cerebral metabolic changes in mice. *J. Neurosci. Res.* **86**, 813–820.
- Jennings K. A., Loder M. K., Sheward W. J. *et al.* (2006) Increased expression of the 5-HT transporter confers a low-anxiety phenotype linked to decreased 5-HT transmission. *J. Neurosci.* **26**, 8955–8964.
- Lapointe N. P., Ung R. V., Bergeron M., Cote M. and Guertin P. A. (2006) Strain-dependent recovery of spontaneous hindlimb movement in spinal cord transected mice (CD1, C57BL/6, BALB/c). *Behav. Neurosci.* **120**, 826–834.
- Laursen T. M., Labouriau R., Licht R. W., Bertelsen A., Munk-Olsen T. and Mortensen P. B. (2005) Family history of psychiatric illness as a risk factor for schizoaffective disorder: a Danish register-based cohort study. *Arch. Gen. Psychiatry* **62**, 841–848.
- Leonardo E. D. and Hen R. (2006) Genetics of affective and anxiety disorders. *Annu. Rev. Psychol.* **57**, 117–137.
- Lewis C. M., Levinson D. F., Wise L. H. *et al.* (2003) Genome scan meta-analysis of schizophrenia and bipolar disorder, part II: Schizophrenia. *Am. J. Hum. Genet.* **73**, 34–48.
- Lucki I. (1998) The spectrum of behaviors influenced by serotonin. *Biol. Psychiatry* **44**, 151–162.
- Mannoury la Cour C., Boni C., Hanoun N., Lesch K. P., Hamon M. and Lanfumey L. (2001) Functional consequences of 5-HT transporter gene disruption on 5-HT_{1A} receptor-mediated regulation of dorsal raphe and hippocampal cell activity. *J. Neurosci.* **21**, 2178–2185.
- Murphy D. L. and Lesch K. P. (2008) Targeting the murine serotonin transporter: insights into human neurobiology. *Nat. Rev. Neurosci.* **9**, 85–96.
- Narbout-Neme N., Pavone L. M., Avallone L., Zhuang X. and Gaspar P. (2008) Serotonin transporter transgenic (SERT^{Cre}) mouse line reveals developmental targets of serotonin specific reuptake inhibitors (SSRIs). *Neuropharmacology* **55**, 994–1005.
- Ozaki N., Goldman D., Kaye W. H., Plotnikov K., Greenberg B. D., Lappalainen J., Rudnick G. and Murphy D. L. (2003) Serotonin transporter missense mutation associated with a complex neuropsychiatric phenotype. *Mol. Psychiatry* **8**, 933–936.
- Parras C. M., Galli R., Britz O. *et al.* (2004) Mash1 specifies neurons and oligodendrocytes in the postnatal brain. *EMBO J.* **23**, 4495–4505.
- Perez J., Mori S., Caivano M., Popoli M., Zanardi R., Smeraldi E. and Racagni G. (1995) Effects of fluvoxamine on the protein phosphorylation system associated with rat neuronal microtubules. *Eur. Neuropsychopharmacol.* **5**(Suppl), 65–69.
- Powell K. J., Hori S. E., Leslie R., Andrieux A., Schellinck H., Thorne M. and Robertson G. S. (2007) Cognitive impairments in the STOP null mouse model of schizophrenia. *Behav. Neurosci.* **121**, 826–835.
- Raponi E., Agenes F., Delphin C., Assard N., Baudier J., Legraverend C. and Deloulme J. C. (2007) S100B expression defines a state in which GFAP-expressing cells lose their neural stem cell potential and acquire a more mature developmental stage. *Glia* **55**, 165–177.
- Robertson G. S., Hori S. E. and Powell K. J. (2006) Schizophrenia: an integrative approach to modelling a complex disorder. *J. Psychiatry Neurosci.* **31**, 157–167.
- Ross C. A., Margolis R. L., Reading S. A., Pletnikov M. and Coyle J. T. (2006) Neurobiology of schizophrenia. *Neuron* **52**, 139–153.
- Shimizu H., Iwayama Y., Yamada K. *et al.* (2006) Genetic and expression analyses of the STOP (MAP6) gene in schizophrenia. *Schizophr. Res.* **84**, 244–252.
- Sun H., Hu X. Q., Emerit M. B., Schoenebeck J. C., Kimmel C. E., Peoples R. W., Miko A. and Zhang L. (2008) Modulation of 5-HT₃ receptor desensitization by the light chain of microtubule-associated protein 1B expressed in HEK293 cells. *J. Physiol.* **586**, 751–762.
- Talbot K., Cho D. S., Ong W. Y. *et al.* (2006) Dysbindin-1 is a synaptic and microtubular protein that binds brain snapin. *Hum. Mol. Genet.* **15**, 3041–3054.

- Tang H., Wang Y., Xie L., Mao X., Won S. J., Galvan V. and Jin K. (2009) Effect of neural precursor proliferation level on neurogenesis in rat brain during aging and after focal ischemia. *Neurobiol. Aging* **30**, 299–308.
- Verge D., Daval G., Marcinkiewicz M., Patey A., el Mestikawy S., Gozlan H. and Hamon M. (1986) Quantitative autoradiography of multiple 5-HT₁ receptor subtypes in the brain of control or 5,7-dihydroxytryptamine-treated rats. *J. Neurosci.* **6**, 3474–3482.
- Vertes R. P. (1991) A PHA-L analysis of ascending projections of the dorsal raphe nucleus in the rat. *J. Comp. Neurol.* **313**, 643–668.
- Vertes R. P., Fortin W. J. and Crane A. M. (1999) Projections of the median raphe nucleus in the rat. *J. Comp. Neurol.* **407**, 555–582.
- Whitaker-Azmitia P. M., Borella A. and Raio N. (1995) Serotonin depletion in the adult rat causes loss of the dendritic marker MAP-2. A new animal model of schizophrenia? *Neuropsychopharmacology* **12**, 269–272.